



ELSEVIER

Physica C 352 (2001) 61–66

PHYSICA C

www.elsevier.nl/locate/physc

Andreev reflection and excess noise in diffusive SNS junctions

C. Strunk^{*}, T. Hoss, C. Schönenberger

Institute of Physics, University of Basel, Klingelbergstrasse 82, CH-4056 Basel, Switzerland

Abstract

We investigated superconductor/normal metal/superconductor (SNS) junctions made of short Au or Cu wires between Nb or Al banks. The Nb based junctions display inherent electron heating effects induced by the high thermal resistance of the NS boundaries. The Al based junctions show in addition subharmonic gap structures in the differential conductance dI/dV and a pronounced peak in the excess noise at very low voltages V . We suggest that the noise peak is caused by fluctuations of the supercurrent at the onset of Josephson coupling between the superconducting banks. At intermediate temperatures where the supercurrent is suppressed a noise contribution $\propto 1/V$ remains, which reflects the strong nonequilibrium of quasiparticles even at very small voltages. © 2001 Elsevier Science B.V. All rights reserved.

PACS: 72.70+m; 73.23.-b; 74.25.Fy; 74.80.Fp

Keywords: Andreev reflection; SNS junctions; Excess noise

1. Introduction

According to the scattering theory of quantum transport, the electrons propagate through mesoscopic conductors between large charge reservoirs similar to photons in wave guides. The conductance is described in terms of transmission modes or transport channels with transmission coefficients \mathcal{T}_n . The discreteness of electrical charge causes current fluctuations, i.e. noise. One obtains the classical shot noise $S_I = 2eI$ in the limit of small transmission $\mathcal{T} \ll \infty$. In this limit the statistics of current fluctuations is Poissonian because transmission is a rare event. As \mathcal{T} increases the statistics crosses over to a binomial distribution which leads to a suppression of the shot noise

$S_I = 2eI(1 - \mathcal{T})$ [1]. In the limit $\mathcal{T} \rightarrow 1$ and temperature $T \rightarrow 0$ the noise vanishes as a consequence of the Pauli principle.

On the other hand, a *diffusive* conductor contains many transport channels whose transmission coefficients obey a *universal* distribution function which favours values of \mathcal{T} close to zero and close to unity [2]. On average this leads to a universal suppression factor of 1/3 with respect to the Poisson limit. The noise suppression in the diffusive limit has been predicted quite long ago [3], but has been only recently verified experimentally [4,5]. Inelastic scattering in the diffusive region leads to a local thermal equilibrium with a current dependent electron temperature exceeding the lattice temperature [6]. The resulting thermal noise averaged over the diffusive region depends also linearly on the current with an equally universal reduction factor of $\sqrt{3}/4$ compared to the Poisson noise. The properties of the reservoirs turned out to be essential for the observed shot noise suppression [5].

^{*} Corresponding author.

E-mail address: christoph.strunk@unibas.ch (C. Strunk).

Several new features are expected, when one or both of the normal conducting reservoirs are replaced by a superconductor. Electrons with energies smaller than the gap energy cannot enter the superconductor because there are no single particle states available. Instead, charge is transferred by the process of Andreev reflection (AR) [7], where a hole is retroreflected at the interface and a Cooper pair enters the superconductor. Since the charge transmitted by an AR is $2e$, the shot noise across single SN interface is doubled as it was confirmed experimentally by Jehl et al. [8] and by Kozhevnikov et al. [9]. When both reservoirs are superconducting, SNS *multiple* Andreev reflections (MAR) are possible, which lead to the formation of Andreev bound states [11] with a minigap of the order of $E_C = \hbar D/L^2$ in the density of states. D and L are the diffusion constant and the length of the normal wire. The Andreev bound states are able to carry a supercurrent at temperatures $k_B T \leq E_C$. At finite voltages, the MAR manifests itself in subharmonic gap structures in the differential conductance [12–15] at voltages $V < 2\Delta/e$ (see Fig. 1).

Low energy quasiparticles are confined to the normal wire, but can leave the junction after $2\Delta/eV$ Andreev reflection because they gain energy by each AR. Hence, the MAR is expected to induce an important broadening of the quasiparticle distribution function when the junction is biased at

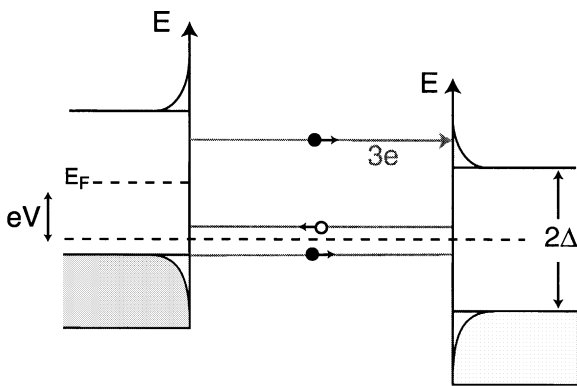


Fig. 1. Schematic of a MAR process between two NS interfaces. Quasiparticles trapped between the SN boundaries can escape into the superconducting banks only if their energy exceeds the energy gap of the superconductor. A charge ne is transferred by the MAR cycle in the voltage range $2\Delta/n < eV < 2\Delta/(n-1)$.

finite voltages. The broadening of the distribution function can be seen as an electron heating effect which is induced by the large thermal resistance of the NS interfaces. We have detected this heating effect by measurements of the voltage fluctuations across the samples which is directly related to the range of partially occupied states in the normal wire [6].

2. Experimental details

The devices were prepared by two-angle shadow evaporation using a novel inorganic Si_3N_4 shadow mask [17]. They consist of thin (≈ 15 nm) Au or Cu wires of 0.4 – 2 μm length and 100 – 200 nm width between thick (50 – 200 nm) Nb or Al reservoirs. The main advantage of this technique is the absence of any organic solvent, which severely degrades the superconducting properties of the highly reactive niobium in small structures patterned with conventional PMMA-based resists. The Si_3N_4 mask is suspended by a 800 nm thick SiO_2 layer above the Si substrate to allow large tilt angle and thus shifts of 1 μm and more between the different shadow images. Because of the excellent mechanical stability of the Si_3N_4 free-standing bridges of several micron length can be fabricated (see Fig. 2).

We investigated the differential conductance dI/dV and the power spectral density S_V of the voltage fluctuations as a function of bias current. The voltage noise across the sample is measured in the frequency range between 100 and 400 kHz with a cross-correlation technique developed earlier [5]. Substantial effort has been taken to shield the sample from external rf interference. All electrical leads into the sample chamber are shielded at room temperature with pi-filters having an attenuation of 70 dB between 25 MHz and 1 GHz. For the voltage leads across the samples the pi-filters would lead to an unacceptable loss in bandwidth and are placed at the output of the first preamplifier located in a rf tight box on top of the cryostat. A thermocoax filtering stage at the sample temperature effectively suppresses noise in the high frequency range above 0.5 GHz, in particular, noise from thermal photons inside the cryostat.

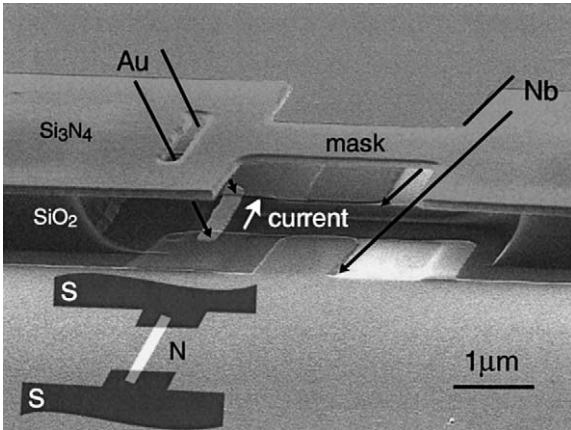


Fig. 2. Scanning electron micrograph of a typical sample viewed under a large tilt angle. The normal wire between the two superconducting reservoirs is defined through the slit in the freely suspended nitride mask. Inset: schematic of the sample layout.

The lossy thermocoax cables are soldered into a rf tight copper can containing the sample. These precautions are essential since our relatively long diffusive junctions have small critical currents, which are easily smeared out by rf interference.

3. Electron heating in Nb/Au/Nb junctions

The differential conductance shown in Fig. 3 of the Nb based junctions displays a sharp peak at zero bias. This dip strongly depends on the ratio L/L_T , where L is the sample length, $L_T = (\hbar D/2\pi k_B T)^{1/2}$ is the thermal diffusion length in the normal metal and D its diffusion constant. For LL_T the peak is relatively small; for $L \approx L_T$ it becomes comparable to the normal state resistance, and for $L < L_T$ a full supercurrent with vanishing resistance is developed. This reflects the exponentially decaying Cooper pair amplitude within the normal wire which is discussed later in more detail. At finite voltages no subharmonic gap structure is observed.

The excess noise of a series of nine Nb/Au/Nb junctions presented in Fig. 4 shows a sharp monotonic rise of S_V at the smallest voltages. At higher voltages the noise increases more moderately. For comparison, Fig. 4 contains also data

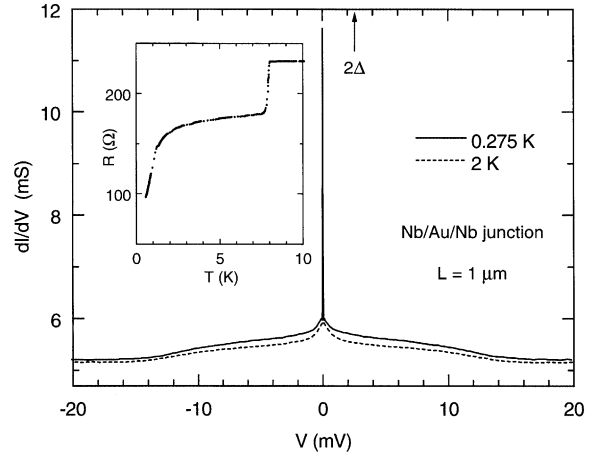


Fig. 3. Differential conductance dI/dV of a single Nb/Au/Nb junction as a function of voltage V for two temperatures. The sharp peak $V = 0$ indicates the rapid destruction of electron-hole coherence by a finite bias voltage. The arrow indicates $V = 2\Delta/e = 2.6$ mV. Note the absence of subharmonic gap structures. The Au wire is $1 \mu\text{m}$ long, 130 nm wide and 15 nm thick. The thickness of the Nb reservoirs is 50 nm. Inset: resistance vs. temperature for the same sample.

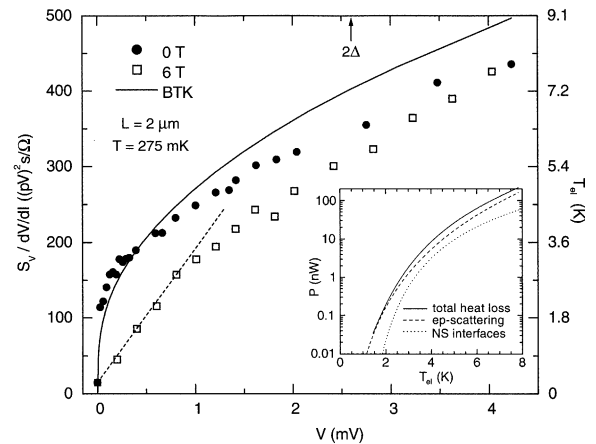


Fig. 4. Scaled excess noise $S_V/dV/dI$ as a function of voltage for a series of 9 Nb/Au/Nb junctions of $2 \mu\text{m}$ length, 200 nm width and 15 nm thickness for normal (\square) and superconducting (\bullet) Nb reservoirs. The arrow indicates $V = 2\Delta/e = 2.6$ mV. The right-hand scale indicates the effective electron temperature. The dashed line indicates the shot noise of noninteracting electrons in case of normal reservoirs. The solid line gives an estimate of the electron heating effect (see text). Inset: electron-phonon (---) and N/S interface (· · ·) contributions to the cooling power as a function of electron temperature T_{ei} in the wire. T_{ei} in the reservoirs is assumed to remain at 0.27 K.

in a magnetic field of 6 T which is sufficient to suppress the superconductivity in the Nb banks. In this case one recovers the expected shot noise $S_I = (1/3) 2eI$ at voltages $V < 1$ mV. At higher voltages electron additional cooling via electron–phonon scattering leads to a negative curvature of S_V [5]. The rapid increase of the noise is interpreted in terms of electron heating effects induced by the high thermal resistance of the NS boundaries. As a consequence of the high gap of the Nb, the electron temperature in the normal wire rises up to several K at voltages of the order of Δ/e . This strong thermal smearing explains also the absence of subharmonic gap structure in dI/dV . The electron heating can be qualitatively described with a slightly modified BTK expression [10] for the heat transfer through the NS interfaces and the electron–phonon scattering. The cooling power for the two contribution is plotted in the inset of Fig. 4.

4. Noise enhancement in Al/Cu/Al junctions

The power dissipation and the corresponding electron heating is much smaller in our Al based samples, because the energy gap is much smaller. In Fig. 5 we show dI/dV curves at different temperatures for a series of $16 \times 1 \mu\text{m}^2$ long Al/Cu/Al junctions. A small supercurrent is found at zero voltage and subharmonic gap structures at voltages V close to integer fractions of $2\Delta/e$. The latter are indicative of MAR. The peak voltages nicely reproduce the temperature dependence of the BCS gap (see right inset in Fig. 1). We observe MAR peaks up to the fourth order. The left inset displays $I(V)$ at the transition to the zero voltage state.

Fig. 6 shows noise data for the same sample as in Fig. 5. The noise is strongly peaked at very low bias voltages and rises linearly at larger voltages. The amplitude of the noise peak is independent of frequency in the range between 100 and 400 kHz [16], which excludes $1/f$ noise. The peak is rapidly suppressed at higher temperatures. At large bias the noise enhancement with respect to normal reservoirs is much less pronounced compared to the Nb/Au/Nb case. This is expected from the lower gap of the Al. In contrast to the Nb based

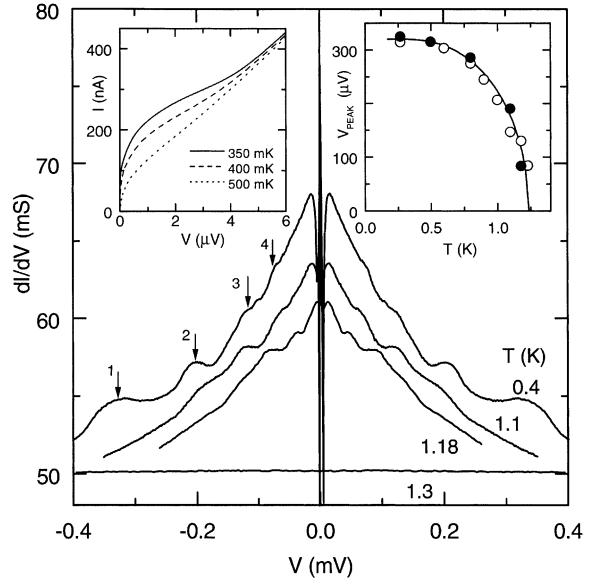


Fig. 5. Differential conductance dI/dV of a series of 16 Al/Cu/Al junctions as a function of voltage V for several temperatures. The arrows indicate subharmonic gap structures corresponding approximately to integer fractions of 2Δ . Left inset: current–voltage characteristics in the low voltage region. Right inset: position of the 2Δ conductance peak vs. temperature for two samples with different normal state conductance (\bullet : 50 mS, \circ : 29.3 mS). The solid line is a BCS fit for $2\Delta = 325 \mu\text{V}$ and $T_c = 1.23$ K.

samples, the nonmonotonic behaviour of the Al based samples cannot be understood as a simple heating effect.

5. Discussion

We believe that the noise peak is related to strong fluctuations of the supercurrent close to the critical current. Because of the exponential decay of the Cooper pair amplitude $F = \langle \psi_\uparrow(x) \psi_\downarrow(x) \rangle \propto \exp(-x/L_T)$ the modulus $|F(x)|$ becomes very weak in the centre of the Cu wire. At this weak spot thermal phase slips are easily excited at currents close to the critical current I_c . The fluctuations of $|F(x)|$ lead to strong temporal fluctuations of the supercurrent.

In other words, the regimes of a true noiseless supercurrent for $I < I_c$ and a dissipative current for I_c are separated by a transition regime where a

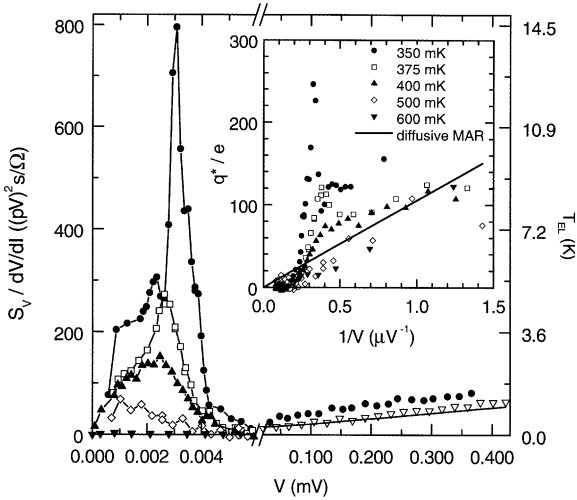


Fig. 6. Scaled excess noise $S_V/dV/dI$ as a function of voltage for the same device as in Fig. 1 with superconducting (●) and normal (▽) reservoirs. The solid line indicates the shot noise of noninteracting electrons in case of normal reservoirs. Note the expanded scale at low V . Inset: effective multiple charge as a function of $1/V$ for the same temperatures. The line indicates the theoretical estimate for q^* for the diffusive case [18].

steady supercurrent cannot be maintained. This leads to the appearance of noise as well as to a finite voltage across the junction which is seen as the rounding of the I - V curves in the left inset of Fig. 5. Our interpretation is supported by the fact that the noise peak rises precisely at the onset of a finite (average) voltage in the I - V characteristics and vanished again in the linear part (see left inset in Fig. 5). With the decay of the supercurrent at elevated temperatures the noise peak also disappears, i.e. the supercurrent noise (like the supercurrent itself) is a short range proximity effect governed by the ratio L/L_T .

Another very interesting issue is the existence of long range phase coherent effects in the noise. Such effects, which persist on the length L_ϕ , have been already observed in the dc conductance [18]. Another long range effect is the presence of MAR peaks in dI/dV in Fig. 5. As the temperature is raised their position changes according to the temperature dependence of the gap Δ , but their amplitude changes remarkably little. One possible effect in the noise is the theoretically predicted formation of multiple charges by the MAR pro-

cess. According to Refs. [19–21] the charge transfer at low voltages $eV \ll \Delta$ is possible only via a large number of Andreev reflections leading to an effective charge $q^* \propto 1/V$. This should result in an enhanced shot noise $S_I = 2q^*I$ at low voltages. The inset of Fig. 6 shows the effective charge $q^*/e = S_I/2eI$ vs. $1/V$. For $T \leq 500$ mK we find a strongly nonlinear behaviour which reflects the peak in S_V . However, at elevated temperatures $T \geq 500$ mK, where the supercurrent is suppressed by thermal fluctuations, we find a roughly linear behaviour with a slope of $\approx 0.3 \times 2\Delta$ consistent with the theory for the diffusive regime [21]. In the latter case, the measured effective charge ranges up to $100e$. This is surprisingly large since the coherence of the MAR cycle is expected to be cut off by inelastic scattering after a few Andreev reflections. More seriously, the noise enhancement appears to vanish at voltages $V = 100 \mu\text{V}$. This contradicts a simple interpretation in terms of multiple charges. In spite of these features, which are currently not completely understood, our experiment indicates the existence of a long range contribution to the noise at low voltages.

Acknowledgements

We thank U. Staufer for providing the Si_3N_4 wafers and T. Nussbaumer and R. Huber for help with the experiments. Useful discussion with C. Bruder, H. Potheir and B. van Wees are gratefully acknowledged. This work was supported by the Swiss National Science Foundation.

References

- [1] A. Kumar, et al., Phys. Rev. Lett. 76 (1996) 2778.
- [2] O.N. Dorokhov, Solid State Commun. 51 (1984) 381.
- [3] C.W.J. Beenakker, M. Büttiker, Phys. Rev. B 46 (1992) 1889.
- [4] R.J. Schoelkopf, P.J. Burke, A.A. Kozhevnikov, D.E. Prober, M.J. Rooks, Phys. Rev. Lett. 78 (1997) 3370.
- [5] M. Henny, S. Oberholzer, C. Strunk, C. Schönberger, Phys. Rev. B 59 (1999) 2871.
- [6] K.E. Nagaev, Phys. Rev. B 52 (1995) 4740.
- [7] A.A. Andreev, JETP 19 (1964) 1228.
- [8] X. Jehl, M. Sanquer, R. Calemczuk, D. Mailly, Nature 405 (2000) 50.

- [9] A.A. Kozhevnikov, R.J. Schoelkopf, D.E. Prober, Phys. Rev. Lett. 84 (2000) 3398.
- [10] G.E. Blonder, M. Tinkham, T.M. Klapwijk, Phys. Rev. B 25 (1982) 4515.
- [11] P.F. Bagwell, R. Riedel, L. Chang, Physica 203 (1994) 475, and the references therein.
- [12] T.M. Klapwijk, G.E. Blonder, M. Tinkham, Physica 109/110B (1982) 1657.
- [13] W.M. van Huffelen, et al., Phys. Rev. B 47 (1993) 5170.
- [14] A.W. Kleinsasser, et al., Phys. Rev. Lett. 72 (1994) 1738.
- [15] E. Scheer, et al., Phys. Rev. Lett. 78 (1997) 3535.
- [16] T. Hoss, et al., Phys. Rev. B, in press.
- [17] T. Hoss, C. Strunk, C. Schönenberger, Microelectronic Engng. 46 (1999) 149.
- [18] H. Courtois, et al., Phys. Rev. Lett. 76 (1996) 130.
- [19] D. Averin, H. Imam, Phys. Rev. Lett. 76 (1996) 3814.
- [20] J.C. Cuevas, A. Martín-Rodero, A. Levy-Yeyati, Phys. Rev. Lett. 82 (1999) 4086.
- [21] Y. Naveh, D.V. Averin, Phys. Rev. Lett. 82 (1999) 4090.